

A New Theory for Interpreting Rate Decline Trends in Solution-Gas Drive Reservoirs

O. MOSOBALAJE

African University of Science & Technology

D. TIAB

University of Oklahoma

Abstract

A number of attempts have been made to establish the theories of rate decline in solution-gas drive reservoirs with multiphase flow. However, none of these attempts have established a functional link between the empirical and the theoretical domains of decline curve analysis for such reservoirs. The absence of such a link has inhibited the formulation of simple techniques for reservoir properties estimation. The purpose of this work is therefore to establish the missing link.

In this work, functional relationships between the empirical b_{emp} and the theoretical b_{th} were derived. The derivation was based on a novel definition of a new parameter known as time-weighted average of the theoretical exponent $\overline{b_{th}}$. This new parameter was found to be related to the empirical exponent b_{emp} , thus establishing the link. A reservoir simulator was used to generate sets of production data used in verifying the derived relationships. Results presented in this paper show that the relationships derived herein are valid, even for heterogeneous reservoirs. The work also offered theoretical justifications for the various ranges of b_{th} values, and for the first time, four distinct rate decline regimes in solution-gas drive reservoirs were identified. Sensitivity analyses were performed on the results. The effects of non-Darcy flow on decline parameters were also investigated.

Lastly, this work provided a mathematical justification for the existence of the hyperbolic family of curves in decline analysis of solution-gas drive reservoirs.

Introduction

Hydrocarbon fields typically show three production phases: the build-up phase, the peak (constant rate) phase and the rate decline phase⁽¹⁾. For a well, during the peak phase, the bottom-hole flowing pressure declines until it reaches a critical value, P_{wfc} . Thereafter, the production rate declines as P_{wfc} is maintained⁽²⁾. Rate decline during the transient behaviour of the drainage area is known as transient rate decline, whereas boundary-dominated decline occurs after the drainage radius has reached the outer boundary⁽³⁾. The empirical decline curve analysis, largely based on Arps⁽⁴⁾ empirical decline models, involves curve-fitting the past production data and extrapolating the curve to predict recoverable reserves and future production rates.

The theoretical approach of decline curve analysis is concerned with investigating the effects of reservoir/fluid properties on the empirical decline model parameters (D_i and b). The essence is to derive functional relationships between the empirical parameters and the reservoir/fluid properties, thereby establishing a theoretical basis for the empirical decline models. Such relationships are useful in formulating techniques for reservoir properties estimation using production data.

Many previous attempts⁽⁵⁻⁸⁾ at establishing functional relationships between the empirical parameters and the reservoir/fluid properties have been concerned primarily with the exponential decline of single phase oil reservoirs. An attempt⁽⁹⁾ to establish the theories of hyperbolic decline of solution-gas drive reservoirs (multi-phase) have yielded an expression relating the decline exponent, b , to reservoir/fluid properties. However, the values (herein termed b_{th}) computed from such theoretical expression, although theoretically sound, are not constant through time as expected. More disturbing is the fact that the b_{th} values did not exhibit any equivalence with the empirically-determined exponent (herein termed b_{emp}). These observations suggest there is a missing link between the theoretical and the empirical domains of decline analysis for solution-gas drive reservoirs.

The objective of this work is therefore to establish the missing link. The work defines a new parameter termed time-weighted average of the values of the theoretical decline parameter, denoted as $\overline{b_{th}}$. Using the new parameter, we derive functional relationships between the empirical parameter, b_{emp} , and the theoretical parameter, b_{th} . This relationship therefore establishes, for the first time, a consistent link between the empirical and the theoretical domains of decline curve analysis for solution-gas drive reservoirs.

The reservoir model considered in this work consists of a fully-penetrating vertical well at the centre of a cylindrical reservoir; flow into the wellbore is assumed to be radial. The reservoir fluid is assumed to be at bubble point. Both homogeneous and heterogeneous reservoir cases are considered. The water phase is assumed immobile; hence a two-phase flow of oil and gas. Rock and water compressibilities are assumed negligible⁽¹⁰⁾. The presence of near-wellbore skin region is considered. A commercial reservoir simulator is used to generate sets of production data used in verifying the derived relationships.

Results of this investigation show that the theoretical parameter b_{th} varies widely through production time. Furthermore, the work offers theoretical justifications for the various ranges of b_{th} values. Hence, it presents for the first time, four distinct rate decline regimes in solution-gas drive reservoirs. Ultimately, the results offer a numerical verification of the functional relationships derived in this work. The relationships are found to be valid, even for heterogeneous reservoirs. Analyses have been performed on the sensitivity of the results to some key parameters. In order to subject the findings of this work to another test, an additional numerical example, adopting a different reservoir model, is provided.

In addition, the effects of non-Darcy flow on decline parameters are investigated. Lastly, a mathematical justification for the existence of the hyperbolic family of curves in decline curve analysis of solution-gas drive reservoirs is provided in this paper.

Literature Background

Several investigators^(9, 11-15) have studied the effects of reservoir/fluid factors on rate decline trends. These factors include relative permeability characteristics, fluid PVT properties, rock properties, wellbore conditions and reservoir drive mechanisms. A number of attempts have also been made to analytically express empirical decline parameters as functions of reservoir/fluid properties. A result of such attempts is the establishment of the fact that the exponential decline is a consequence of single phase slightly compressible liquid production^(2, 5). Guo et al.⁽²⁾ derived the exponential decline equation by combining the pseudo-steady state flow equation for a volumetric reservoir with the single phase material balance equation. Fetkovich⁽⁵⁾, using a combination of material balance equations and oil well rate-pressure relationships, derived an exponential rate-time relationship for single phase flow. Consequently, he developed an expression for the empirical parameter, D_i , in terms of reservoir/fluid properties. Additionally, Fetkovich⁽⁵⁾ combined the analytical solution of the transient period with empirical solution of the boundary-dominated period to develop a unified semi-analytical decline type curve.

Camacho and Raghavan⁽¹⁶⁾ proposed solution-gas pseudo-pressure and pseudo-time functions with which they correlated multi-phase solution-gas drive systems with single phase slightly compressible liquid systems. Using the pseudo functions, Camacho and Raghavan⁽⁹⁾ provided a theoretically rigorous derivation of the decline parameters (D_i and b) as follows:

$$D_i = \frac{2\pi \cdot 0.006328k \left(\frac{\bar{\lambda}_T}{\bar{c}_T} \right)}{D\phi A} \dots\dots\dots (1)$$

$$b_{th} = \frac{D\phi A}{2\pi \cdot 0.006328k} \frac{d}{dt} \left(\frac{\bar{c}_T}{\bar{\lambda}_T} \right) \dots\dots\dots (2)$$

On the basis of the equations above, the authors discussed the theoretical implications of Arps' model thus:

If the ratio $\bar{\lambda}_T / \bar{c}_T$ is approximately constant through time, then the rate data would fit to the Arps' exponential decline ($b = 0$). On the other hand, If the ratio $\bar{\lambda}_T / \bar{c}_T$ is a linear function of time, then the rate data would fit to a unique member of the hyperbolic family ($b = constant$).

However, the authors observed from their simulation studies that the ratio $\bar{\lambda}_T / \bar{c}_T$ varies non-linearly with time. They also noted that the parameter b is not constant in most of the theoretical studies.

Theoretical Derivations

The theories derived in this work are presented in two sections; the foremost being the derivation of functional relationships between the empirical domain and the theoretical domain. This work also derived a new expression, b_{th} , incorporating near-wellbore non-Darcy flow.

Derivation of Relationship

Here, the empirical domain is represented by Arps'⁽⁴⁾ general equation:

$$\frac{1}{q} \frac{dq}{dt} = aq^{b_{emp}} \dots\dots\dots (3)$$

On the other hand, the theoretical domain is represented by Equations (1) and (2) above.

Until now, it has been expected that the two parameters above (b_{th} and b_{emp}) are equivalent. This expectation was expressed in reference 9 suggesting the physical phenomena that could yield a constant value of b_{th} equivalent to a given value of b_{emp} . However, simulations carried out in this current work yielded values of b_{th} that varied considerably with time and exhibited no equivalence to b_{emp} . Worse still, an attempt (based on a false expectation of 'equivalence') to import the empirically-determined b_{emp} into Equation (2) in order to solve for permeability, k , yielded spurious results. These observations suggest a missing link between the empirical and the theoretical domains.

In the search for the missing link, this work conceptualized and defined a new parameter known here as the *time-weighted average of the values of the theoretical decline parameter*, denoted as \bar{b}_{th} . Thus,

$$\bar{b}_{th} = \frac{\sum_{t_o}^t (b_{th} \times \text{incremental time elapsed})}{\text{Total Time elapsed since decline started}}$$

For example,

$$\bar{b}_{th} = \frac{\sum_{t_o}^{t_i} \{ b_{th} \times [t_{(i)} - t_{(i-1)}] \}}{t_{(i)} - t_{(o)}} \dots\dots\dots (4)$$

Using this newly-defined parameter, we derive a functional relationship between b_{emp} and \bar{b}_{th} . By replacing the summation term in Equation (4) with an integral term [since b_{th} varies with time, i.e. $b_{th} = f(t)$], and substituting Equation (2) into the resulting expression, the following is obtained:

$$\bar{b}_{th} = \frac{\int_{t_o}^{t_i} \frac{\phi A}{2\pi \cdot 0.006328k} D \frac{d}{dt} \left(\frac{\bar{c}_T}{\bar{\lambda}_T} \right) dt}{t_{(i)} - t_{(o)}}$$

Therefore,

$$\bar{b}_{th} = \frac{\phi AD}{2\pi \cdot 0.006328k} \left(\frac{\bar{c}_T}{\bar{\lambda}_T} \right) \dots\dots\dots (5)$$

Combining Equation (1) with Arps' exponential equation yields the following expression.

$$\frac{1}{q} \frac{dq}{dt} = \frac{2\pi \cdot 0.006328k \left(\frac{\bar{\lambda}_T}{\bar{c}_T} \right)}{D\phi A} \dots\dots\dots (6)$$

Upon substituting Equation (6) into Equation (5) and rearranging the terms, the equation below is obtained:

$$\frac{1}{q} \frac{dq}{dt} = \frac{1}{b_{th}(t_{(i)} - t_{(o)})} \dots\dots\dots (7)$$

Finally, substituting Equation (3) into Equation (7) yields the anticipated relationship. Thus

$$\frac{1}{b_{th}(t_{(i)} - t_{(o)})} = aq^{b_{emp}} \dots\dots\dots (8)$$

TABLE 1: Reservoir properties data set.

Reservoir Properties	Values
Drainage Radius, r_e (ft)	2,624.672
Porosity, ϕ (fraction)	0.3
Permeability, K (mD)	10
Well Radius, r_w (ft)	0.32808
Initial Reservoir Pressure, P_i (psi)	5,704.78
Skin Factor, s	10
Initial Water Saturation, S_{wi} (fraction)	0.3
Reservoir Temperature, T_F (°F)	220
Gas gravity, γ_g	0.65
Oil gravity, γ_{API}	45.5
Thickness, h (ft)	15.55
Critical Bottomhole Pressure, P_{wfc} (psi)	1,696

Equation (8) presents, for the first time, the anticipated link between the empirical and the theoretical domains of decline curve analysis for solution-gas drive reservoirs.

Further still, upon rearranging Equation (5), we represent the LHS of Equation (8) in another form as follows:

$$\frac{1}{b_{th}(t_i - t_o)} = \frac{2\pi \cdot 0.006328k \cdot \bar{\lambda}_T}{\phi AD \bar{c}_T} \dots\dots\dots (9)$$

Equations (8) and (9) have the same LHS quantity. The RHS of Equation (8) represents the empirical, while the RHS of Equation (9) represents the theoretical equivalence of the common LHS. The approximate equivalence of the two RHS terms is the subject of the section ‘Verification of Theories’ presented below.

To the best of our knowledge, these relationships derived here have not been presented before now and are therefore significant contributions to this body of work.

Non-Darcy Considerations

The derivation of the b_{th} expression in Equation (2) in reference 9 did not take the near-wellbore non-Darcy flow (turbulence) into consideration. This work, therefore, derives a new expression for b_{th} with considerations for near-wellbore non-Darcy flow effects as follows:

$$b_{th-nD} = \frac{\phi A}{2\pi \cdot 0.006328k} \left[N \frac{d}{dt} \left(q_{fg} \frac{\bar{c}_T}{\lambda} \right) + D \frac{d}{dt} \left(\frac{\bar{c}_T}{\lambda} \right) \right] \dots\dots\dots (10)$$

Note that Equation (10) only holds if $\frac{2\pi \bar{r}_{AD}}{(D + Nq_{fg})} < 1$.

The details of the derivation of Equation (10) are presented in the Appendix of this paper.

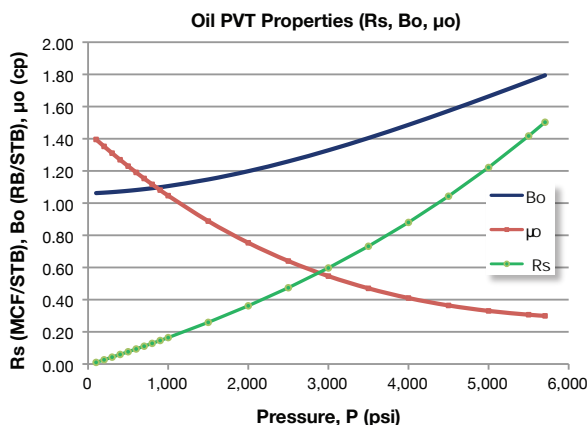


FIGURE 1a: Oil PVT properties.

Verification of Theories

Essentially, the theories developed in this work are presented as Equations (8), (9) and (10). The verification of the equivalence of the two RHS terms of Equations (8) and (9) is the subject of this section. A commercial simulator was utilized to generate sets of production data used in verifying the derived relationships.

Simulation Model and Computations

The reservoir model published in reference 9 is essentially adopted here. The reservoir properties, fluid PVT properties and the relative permeability characteristics are presented in Table 1 and Figures 1a, 1b and 2. The relative permeability data were imparted to the simulator as two-point saturation functions. In order to replicate reality, the simulation was initially placed on a constant well rate control (representing the peak phase). Upon attainment of P_{wfc} , the simulator is made to switch to constant BHP control (representing the decline phase). The peak rate was set at 70% of AOF, as suggested by Fraim and Wattenbarger⁽¹⁷⁾. Parameters relevant to the verification of the derived relationships were included in the simulation output request. The simulation report time-step was set at 1 month, however, the month wherein decline started was expanded into days to improve accuracy. The simulation coordinate was radial with dimensions 10, 1, 2 (r, θ, z).

Additionally, the total compressibility, \bar{c}_T , and mobility, $\bar{\lambda}_T$, terms which were not obtainable directly from simulation outputs were obtained using the outputs in the following computational schemes:

$$\bar{c}_T = \frac{\bar{S}_o}{B_o(\bar{P})} \left[\frac{dB_o(\bar{P})}{d\bar{P}} - B_g(\bar{P}) \frac{dR_s(\bar{P})}{d\bar{P}} \right] - \frac{\bar{S}_g}{B_g(\bar{P})} \left[\frac{dB_g(\bar{P})}{d\bar{P}} \right] \dots\dots\dots (11)$$

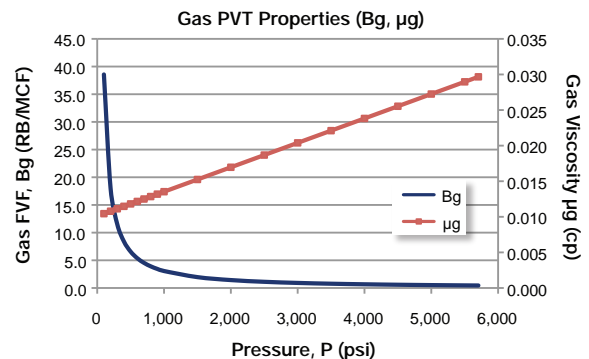


FIGURE 1b: Gas PVT properties.

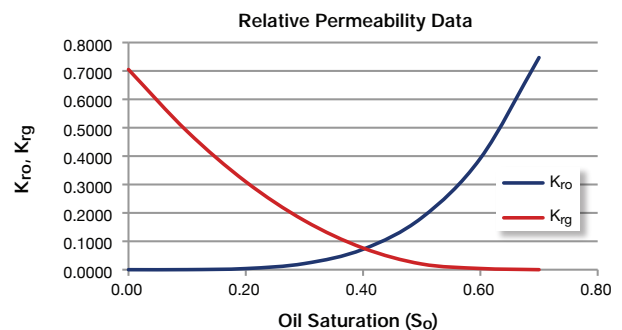


FIGURE 2: Relative permeability characteristic curves.

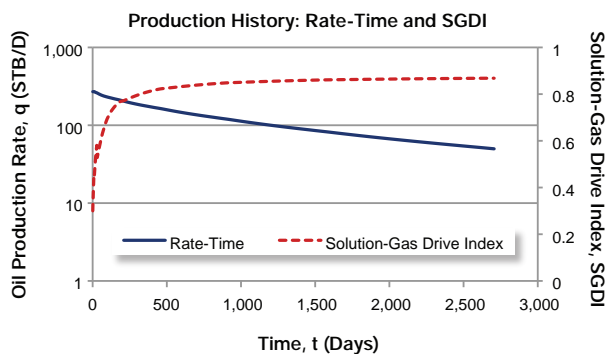


FIGURE 3: Base Case production history: rate-time and SGDI.

$$\bar{\lambda}_T = \frac{k_{ro}(\bar{S}_o)}{\mu_o(\bar{P})} + \frac{k_{rg}(\bar{S}_g)}{\mu_g(\bar{P})} \dots\dots\dots (12)$$

The fluid properties as well as the relative permeability data, as functions of time, were evaluated at average reservoir pressure and saturations using the curve-fit functions generated from the raw input data. The derivatives, as functions of time, were computed using the moving least-square polynomial algorithm. For example:

$$\frac{dB_o(\bar{P})}{d\bar{P}} = \frac{\frac{B_{o(i)} - B_{o(i-1)}}{\bar{P}_{(i)} - \bar{P}_{(i-1)}} [\bar{P}_{(i+1)} - \bar{P}_{(i)}] + \frac{B_{o(i+1)} - B_{o(i)}}{\bar{P}_{(i+1)} - \bar{P}_{(i)}} [\bar{P}_{(i)} - \bar{P}_{(i-1)}]}{\bar{P}_{(i+1)} - \bar{P}_{(i-1)}} \dots\dots\dots (13)$$

The empirical parameters *a* and *b_{emp}* were computed using the simulation output of rate-time data in conventional graphical techniques.

Results

The production rate-time data as generated by the simulation is presented in Figure 3. The slight upward curvature of the semi-log rate-time plot confirms the presence of hyperbolic rate decline, as suggested in reference 10. Additionally, Figure 3 presents the fraction of production due to solution-gas drive mechanism (SGDI). This result confirms the dominance of solution-gas drive mechanism.

The result of the verification attempt is presented in Figure 4 as a plot of the RHS of both Equations (8) and (9) with time. It is observed that the empirical and the theoretical curves exhibited similar trends over time. The initial agreement between the two

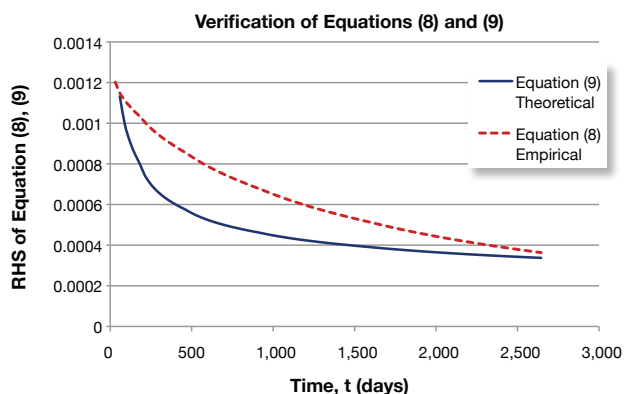


FIGURE 4: Base Case verification of Equations (8) and (9).

curves may be taken as a pseudo agreement since the empirical domain cannot exist until there is a substantial production decline history. It is also observed that the agreement between the two curves improves with time (92.3% at the end of simulation). The significance of these results in formulating techniques for reservoir properties estimation, is the subject of an ongoing investigation to be published in a companion paper.

Theoretical Justifications for Rate Decline Trends

The values of the theoretical parameter, *b_{th}*, computed at each time node of the simulation output using Equation (2) are presented in Figure 5.

From Figure 5, it is obvious that the *b_{th}* ranges from values greater than 1.0 to values as low as 0.33. As a precursor to the explanations offered below for the various intervals of values, this work suggests that the theoretical *b_{th}* values should be seen as reflecting the actual dynamics of the reservoir-fluid interaction through time. Hence, it may be expected to have a dynamic (unstable) behaviour through time, contrary to expectations of a constant *b_{th}* value. Below is a theoretical explanation offered by this work for the various intervals of values of *b_{th}*.

a) *b_{th}* > 1.0: Transient Rate Decline Regime

This range of values may be attributed to transient rate decline, i.e. a decline period during which the pressure pulse is yet to reach the external boundary of the drainage area. Various researchers^(5,6,9) have suggested that decline data existing in the transient period will yield values of exponent *b* greater than 1.0. As evidence in support of this proposition, results presented in the sensitivity analysis section of this paper showed that this range of values vanished for cases that excluded transient rate decline.

b) 1 > *b_{th}* > 0.67: Transition Rate Decline Regime

Empirical surveys^(5,6,9) have shown that the exponent *b* should range from 0.33 to 0.67 for solution-gas drive reservoirs. However, this work suggests there should be a sort of transition regime between the transient rate decline regime, *b_{th}* > 1.0, (if present) and the solution-gas drive decline regime, 0.67 > *b_{th}* > 0.33. In other words, the values between 1.0 and 0.67 in Figure 5 may be seen as representing a transition from transient rate decline regime to solution-gas drive rate decline regime. As expected, results presented in the sensitivity analysis section of this

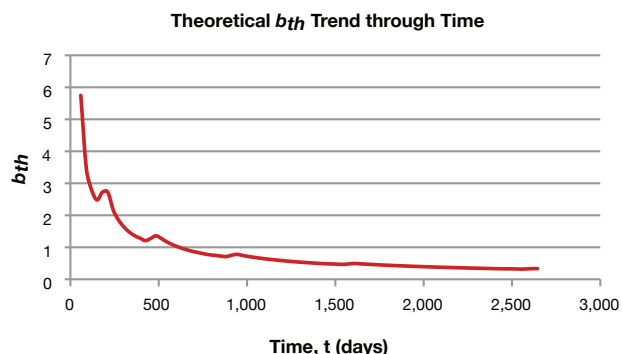


FIGURE 5: Base Case: theoretical *b_{th}* trend through time.

paper showed that this range of values vanished for cases that excluded transient rate decline.

c) $0.67 > b_{th} > 0.33$: Solution-gas Drive Rate Decline Regime

The values in this range should represent the actual boundary-dominated solution-gas drive rate decline behaviour. This fact could be supported by the fact that the reservoir exhibited this range of values for the longest period of the decline phase.

d) $b_{th} < 0.33$: Approaching Single-Phase Production

Some cases considered and reported on in later sections of this paper, exhibited a range of b_{th} values less than 0.33. These values are below the empirically expected range for solution-gas drive reservoirs. Our opinion is that, as the reservoir loses more of the solution-gas due to production, its behaviour starts to approach that of a slightly compressible liquid single-phase flow. Single-phase slightly compressible liquid flows are known theoretically to decline exponentially, i.e. $b = 0$ ^(2,10). Hence, as the reservoir approaches single-phase flow behaviour, the b_{th} values are seen to be less than 0.33 and are approaching zero.

To the best of our knowledge, the identification of these four distinct rate decline regimes in solution-gas drive reservoirs have not been presented previously and is therefore a significant contribution to this work.

The Influence of Non-Darcy Flow

Camacho and Raghavan⁽⁹⁾ had expressed hopes that the incorporation of near wellbore non-Darcy flow effects into the theoretical developments of rate decline in solution-gas drive reservoirs could yield constant values of b_{th} throughout decline time. In order to verify this expectation, we computed values of b_{th-nD} (theoretical decline parameter with consideration for non-Darcy flow) using Equation (10). The result is presented in Figure 6, on the same axes with values of b_{th} for comparison.

From Figure 6, it is evident that the decline parameter with consideration for non-Darcy effects, b_{th-nD} , vary through time much same way as the decline parameter without consideration for non-Darcy effects, precluding any tendency for constant values of b_{th} through time.

If the propositions about the dynamic behaviour of the theoretical decline parameter as being presented by this work are valid, then the b_{th-nD} values may never exhibit any constancy in spite of considerations for non-Darcy flow effects. The b_{th} values will rather be expected to reflect the dynamics (through time) of the reservoir-fluid interactions (mobility/compressibility). System mobility (relative permeability and viscosity) as well as com-

pressibility (PVT) in solution gas drive reservoirs are known to be functions of average reservoir pressure and saturation which change with time due to production.

The exponent b has been related to the popular back-pressure curve exponent⁽¹⁰⁾ denoted as n . Fetkovich⁽¹⁸⁾ had attributed exponent n values less than unity to non-Darcy flow. Camacho and Raghavan⁽¹⁹⁾ also published results that substantiated Fetkovich's claims. However, Fetkovich⁽¹⁸⁾ submitted that n values can be less than unity strictly as a result of variation in fluid properties. As a matter of fact, Camacho and Raghavan⁽¹⁹⁾ suggest that n values will generally vary with time unless the variation is completely counteracted with the non-Darcy flow effects. However, non-Darcy flow coefficients in solution gas drive reservoirs are very small in value (1.71×10^{-6} D/MCF) for the reservoir/fluid model considered here, and may never measure up to values sufficient to counteract the variations due to changes in fluid properties. The results in this work confirm the positions already established in the literature.

Sensitivity Analysis

The following analyses were performed with the aim of establishing the effect of changing some key parameters on the results obtained in this work. In each case, the value for a parameter is changed and the result is compared to the base case.

Case 1: Effect of Permeability Value

The essence of this case study is to create a reservoir model that precludes the occurrence of transient rate decline. It is expected that the higher the absolute permeability of the reservoir rock, the faster the pressure pulse travels to the external boundary of the drainage area. Hence, the more the likelihood of boundary-dominated flow setting in ahead of the onset of decline phase, thereby precluding transient rate decline. For this case, the absolute permeability of the reservoir model was set at 100 mD as against 10 mD in the base case. Also, to accommodate the increased permeability, the peak rate was set at 1,000 STB/D as against 270 STB/D in the base case.

The result of this case study is presented in Figure 7 as a plot of b_{th} values through time. This result was found to conform to expectations as the b_{th} values obtained were less than 1.0, thereby confirming the absence of transient rate decline. Of course, if indeed the transient rate decline regime was absent, then it is only proper to expect that the transition regime (between transient and solution-gas drive rate decline regimes) also be absent. The results of this case study also confirmed the absence of the transition decline regime since the b_{th} interval $1 > b_{th} > 0.67$ was absent. This result, therefore, lends credence to the correctness of the theoretical justifications offered by this work for the various intervals of b_{th} values.

Case 2: Effect of Reservoir Drainage Radius

As in case 1 above, the essence of this case study is to create a reservoir model that precludes the occurrence of transient rate decline. It is expected that the smaller the well's drainage area, the sooner the pressure pulse reaches the external boundary of the drainage area. Hence, the more the likelihood of boundary-dominated flow setting in ahead of the onset of decline phase, thereby precluding transient rate decline. For this case, the external radius of the reservoir model was set at 1,000 ft as against 2,624.672 ft in the base case. Also, to maintain the intended res-

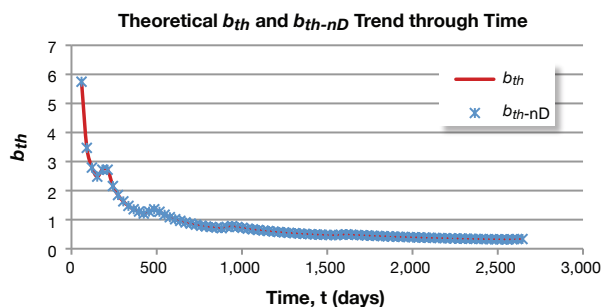


FIGURE 6: Base Case: theoretical b_{th} and b_{th-nD} trend through time.

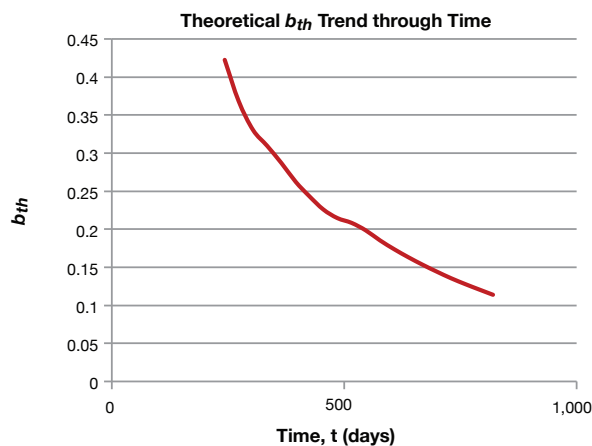


FIGURE 7: Case 1: theoretical b_{th} trend through time.

ervoir pore volume, the reservoir thickness was set at 107 ft as against 15.55 ft in the base case.

The result of this case study is presented in Figure 8 as a plot of b_{th} values through time. This result was found to conform to expectations as both the transient rate decline regime ($b_{th} > 1.0$) and the transition rate decline regime ($1 > b_{th} > 0.67$) were absent. Again, this lends credence to the validity of the theoretical justifications offered by this work for the various intervals of b_{th} values.

Case 3: Effect of Peak/Initial Rate

The peak rate (rate at onset of decline) is a measure of the reservoir/wellbore capacity. The essence of this case study is to investigate the effect that factors such as wellbore diameter and wellhead pressure requirements may have on the results of this work. For this case, the peak rate was set at 200 STB/D (about 50% of the AOF) as against 270 STB/D (about 70% of the AOF) in the base case. Lowering the peak rate this way resulted in a delay of the onset of decline for about 246 days (from 12 days in the base case to 258 days in this case). This is expected since producing at a lower rate requires a lower pressure drawdown; hence, the attainment of the critical bottomhole pressure is delayed. Moreover, a lower rate is expected to be sustained longer.

The result of this case study is presented in Figure 9 as a plot of b_{th} values through time. From the plot it is observed that the maximum (and initial) value of the theoretical b_{th} was 1.88 as against 5.74 for the base case. This is arguably due to the delayed onset of the decline phase. Since decline is delayed, it is expected that

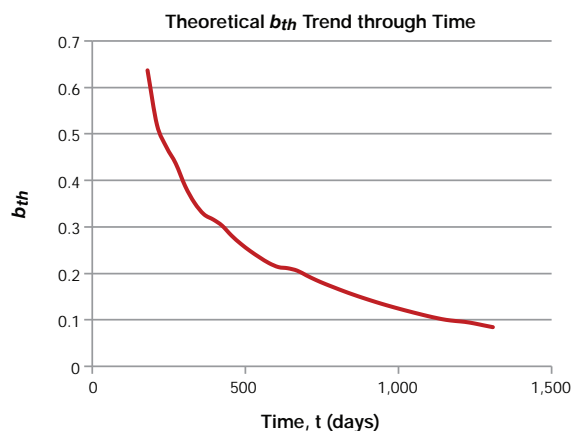


FIGURE 8: Case 2: theoretical b_{th} trend through time.

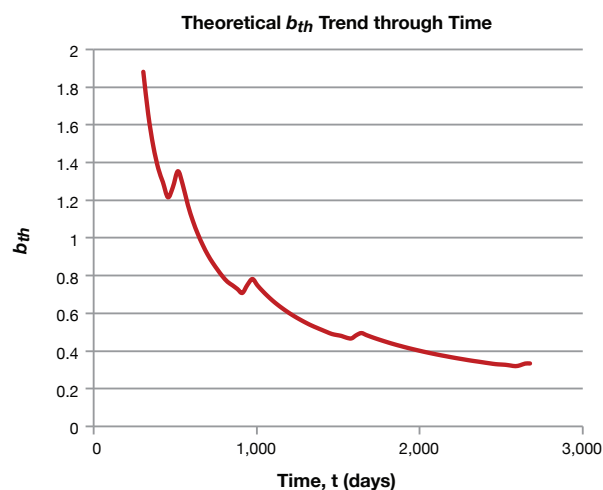


FIGURE 9: Case 3: theoretical b_{th} trend through time.

there will be less of a transient rate decline regime as the onset of decline might have occurred nearer the beginning of boundary dominated flow. This result suggests that the more transient rate decline regime experienced by a well, the higher above 1.0 will be its initial b_{th} values.

Case 4: Effect of Critical Bottomhole Pressure

The essence of this case study is to investigate the effect of the critical bottomhole pressure on the theoretical decline parameter, b_{th} , as well as on the agreement between the empirical and the theoretical curves represented by Equations (8) and (9), respectively. The critical bottomhole pressure is a function of wellbore performance and reservoir deliverability. In this case, the critical bottomhole pressure was set at 700 psi as against 1,696 psi in the base case.

The result of this case study is presented in Figure 10 as a plot of b_{th} values through time. It is noted that the lowest value of b_{th} recorded is about 0.4. This suggests the condition in the reservoir is still far from being considered to be approaching single phase behaviour, i.e. the reservoir has not yet exhausted the time span for the solution-gas rate decline regime. This fact is arguably the reason for the reduced agreement between the empirical and the theoretical curves, even at field abandonment as shown in Figure 11.

Case 5: Effect of Heterogeneity

The essence of this case is to investigate the effect of reservoir heterogeneity (permeability and porosity) on the agreement between the empirical and the theoretical curves represented by Equations (8) and (9), respectively. For this case, the reservoir model as described in the base case was divided into two layers. Heterogeneity was introduced into the reservoir simulation model by assigning different values of porosity and permeability to different layers according to the grid data shown in Table 2. Two heterogeneous cases were considered in order to investigate, not just the effect of heterogeneity, but also the effect of the degree of heterogeneity. For the purpose of comparison, the values of properties assigned to each heterogeneous case is such that the thickness-weighted average permeability and the thickness-weighted average porosity are still the same values as the permeability and porosity values in the base case.

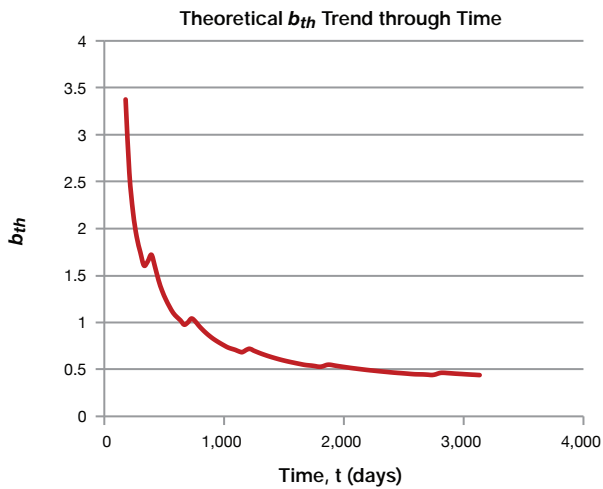


FIGURE 10: Case 4: theoretical b_{th} trend through time.

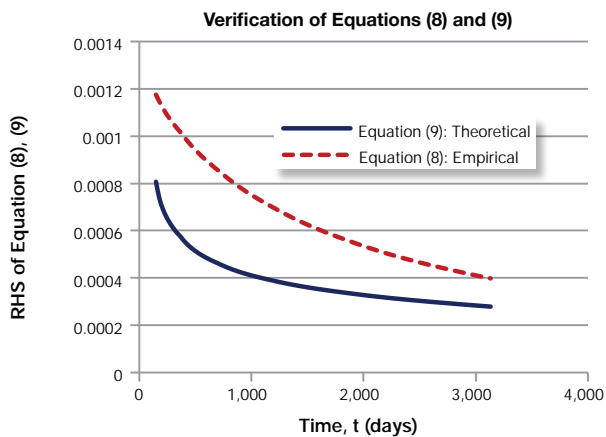


FIGURE 11: Case 4: verification of Equations (8) and (9).

The results of these heterogeneous cases are presented in Figures 12 and 13 as plots of the RHS of both Equations (8) and (9) with time. The results showed that generally, there is an agreement between the empirical and the theoretical domains, even for heterogeneous reservoirs. Furthermore, the results showed that the degree of agreement reduces with increasing heterogeneity. Note that Case 5a (Figure 12) has a higher degree of heterogeneity (layer 1: 150 mD; layer 2: 50 mD) than Case 5b (Figure 13) (layer 1: 130 mD; layer 2: 70 mD).

Additional Example

In order to subject the findings of this work to another test, an additional numerical example, adopting a different reservoir

TABLE 2: Grid data for heterogeneous case.

Case 5a			
	Thickness	Permeability	Porosity
Layer 1	8	150	0.35
Layer 2	7.55	50	0.25
Thickness-weighted Average		101.45	0.301
Case 5b			
	Thickness	Permeability	Porosity
Layer 1	8	130	0.35
Layer 2	7.55	70	0.25
Thickness-weighted Average		100.87	0.301

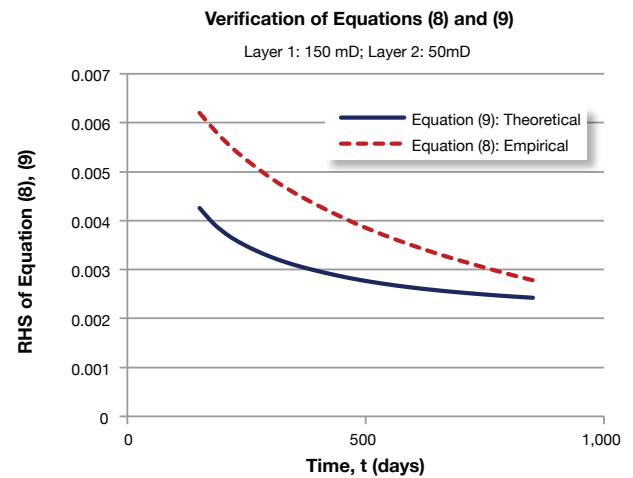


FIGURE 12: Case 5a: verification of Equations (8) and (9).

model, is provided. The reservoir model adopted here is that published by Frederick and Kelkar⁽²⁰⁾, except for the relative permeability data, in which case the data for the first reservoir model is retained. Again, the commercial simulator was used to generate a set of declining production data.

The result for this additional example is presented in Figure 14 as plots of the RHS of both Equations (8) and (9) with time. Again, the results showed excellent agreement between the empirical and the theoretical domains of decline curve analysis for solution-gas drive reservoirs.

Mathematics of the Existence of Hyperbolic Family of Curves in Solution-Gas Drive Reservoirs

This work also presents a mathematical justification for the existence of the hyperbolic family of curves in decline curve analysis of solution-gas drive reservoirs. This approach is based on a novel concept of inner boundary condition (i.e. constant wellbore pressure) of the diffusivity equation in terms of solution-gas pseudo-pressure and pseudo-time functions.

The approach here employed the dimensionless solution-gas pseudo functions presented by Camacho and Raghvan^(9,16) as follows.

At the wellbore, the dimensionless pseudo-pressure is thus:

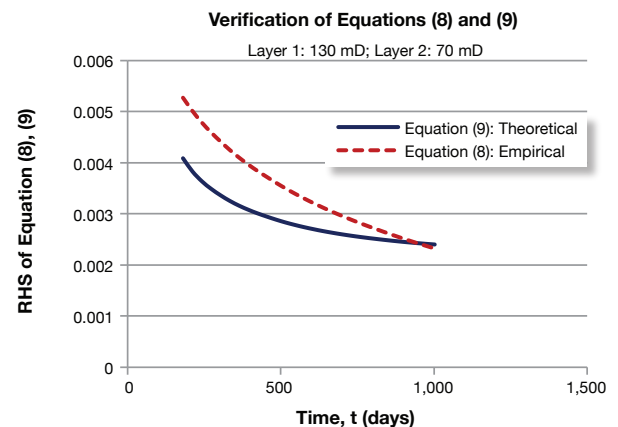


FIGURE 13: Case 5b: verification of Equations (8) and (9).

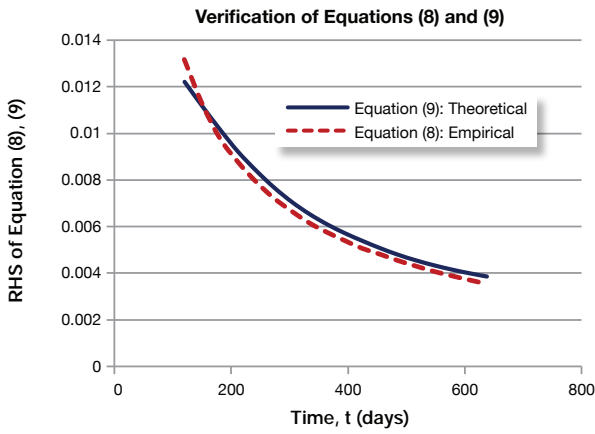


FIGURE 14: Additional example: verification of Equations (8) and (9).

$$P_{p_w D}(r_w, t) = \frac{kh}{141.2q(t)} \left[\int_{P_w}^{\bar{P}(t)} \left(\frac{K_{ro}}{\mu_o B_o} \right) dP + \int_{\bar{P}(t)}^{P_i} \left(\frac{K_{ro}}{\mu_o B_o} \right) dP \right] \dots\dots\dots (14)$$

The dimensionless pseudo-time functions are

$$\tilde{t}_{AD} = \frac{0.006328k}{\phi A q(t)} \int_0^t \frac{q(t) \bar{\lambda}_T(t)}{\bar{c}_T(t)} dt \dots\dots\dots (15)$$

$$\bar{t}_{AD} = \frac{0.006328k}{\phi A} \int_0^t \frac{\bar{\lambda}_T(t)}{\bar{c}_T(t)} dt \dots\dots\dots (16)$$

Equation (16) is only applicable for constant rate cases.

To derive the inner-boundary condition in terms of these dimensionless pseudo-functions, this work considers that:

$$P_{pD(r_D=1,t)} = \frac{kh}{141.2q(t)} \left[\int_{P_w}^{\bar{P}(t)} \left(\frac{K_{ro}}{\mu_o B_o} \right) dP + \int_{\bar{P}(t)}^{P_i} \left(\frac{K_{ro}}{\mu_o B_o} \right) dP \right] \dots\dots\dots (17)$$

It has been shown⁽¹⁶⁾ that the following relationship, first published by Fetkovich⁽¹⁸⁾, is valid for boundary dominated flow in solution-gas drive reservoirs:

$$q_o = \frac{kh}{141.2 \left(\ln \frac{r_e}{r_w} - 0.75 + s \right)} \int_{P_w}^{\bar{P}(t)} \left(\frac{K_{ro}}{\mu_o B_o} \right) dP \dots\dots\dots (18)$$

Substituting Equation (18) into Equation (17), the following expression was obtained:

$$P_{pD(r_D=1,t)} = \left(\ln \frac{r_e}{r_w} - 0.75 + s \right) + \left[\frac{kh}{141.2q(t)} \int_{\bar{P}(t)}^{P_i} \left(\frac{K_{ro}}{\mu_o B_o} \right) dP \right]$$

The group $(\ln \frac{r_e}{r_w} - 0.75 + s)$ is denoted as D , therefore

$$P_{D(r_D=1,t)} = D + \left[\frac{kh}{141.2q(t)} \int_{\bar{P}(t)}^{P_i} \left(\frac{K_{ro}}{\mu_o B_o} \right) dP \right] \dots\dots\dots (19)$$

It has also been shown⁽⁹⁾ that the dimensionless pseudo-pressure corresponding to the average reservoir pressure \bar{P}_{pD} for constant wellbore production mode can be expressed as either a function of \tilde{t}_{AD} or \bar{t}_{AD} as follows:

$$\bar{P}_{pD} = \frac{kh}{141.2q(t)} \int_{\bar{P}(t)}^{P_i} \left(\frac{K_{ro}}{\mu_o B_o} \right) dP = 2\pi \tilde{t}_{AD} \dots\dots\dots (20)$$

$$\bar{P}_{pD} \equiv -D \left[1 - \exp \left(\frac{2\pi \bar{t}_{AD}}{D} \right) \right] \dots\dots\dots (21)$$

Substituting Equation (21) into Equation (19) yields

$$P_{D(r_D=1,t)} = D + -D \left[1 - \exp \left(\frac{2\pi \bar{t}_{AD}}{D} \right) \right]$$

Further simplification yields the following final expression.

$$P_{D(r_D=1,t)} = D \exp \left(\frac{2\pi \bar{t}_{AD}}{D} \right) \dots\dots\dots (22)$$

This work therefore presents Equation (22) as the derived expression of the inner boundary condition (constant wellbore pressure) for solution-gas drive reservoirs (multiphase flow). To the best of our knowledge, this expression has not been presented before now and is therefore a significant contribution to this work.

The inner boundary condition (constant wellbore pressure) for single-phase slightly compressible liquid flow in dimensionless form is commonly represented mathematically as follows⁽²¹⁾:

$$P_{D(r_D=1,t)} = 1 \dots\dots\dots (23)$$

This approach then provides the mathematical justification for the existence of the hyperbolic family of curves in the rate decline curve analysis of solution-gas drive reservoirs by making a comparison of Equations (22) and (23), as follows:

1. From the RHS of Equation (23), it is clear that the inner boundary condition for the single phase slightly compressible case is uniquely defined with a constant value of 1.0. Hence, the diffusivity equation would yield a unique solution corresponding to the exponential decline curve ($b = 0$). It has been shown theoretically⁽⁵⁾ that the exponential decline curve is the late-time, constant wellbore pressure solution of the diffusivity equation.
2. From the RHS of Equation (22), it is noted that the inner boundary condition for the solution-gas drive reservoir is not uniquely defined (even for a given reservoir model). Rather, the expression is a function of fluid properties, $\left\{ \bar{t}_{AD} = f \left[\frac{\bar{c}_T(t)}{\bar{\lambda}_T(t)} \right] \right\}$. Hence, solving the diffusivity equation

with Equation (22) as the inner boundary condition would yield a family of curves (hyperbolic family $0 < b \leq 1.0$) with each member of the family (a given value of b) only uniquely defined for a unique fluid model.

In summary, this work submits that the hyperbolic decline behaviour of solution-gas drive reservoirs is a direct consequence of the inner boundary condition (constant wellbore pressure) of the dimensionless diffusivity equation for solution-gas drive reservoirs.

From the foregoing, it is observed that the ratio $\bar{c}_T(t) / \bar{\lambda}_T(t)$ would be a significant determinant of the value of b for a given

reservoir/fluid model. This observation is in agreement with results published by Gentry and McCray⁽¹¹⁾ showing that the relative permeability characteristics have a significant influence on the parameter b . This is also in agreement with the expression for parameter b presented in Reference (9).

This mathematical justification for the existence of the hyperbolic family of curves in rate decline analysis of solution-gas drive reservoirs is a major contribution to this work.

The significance of this derivation, shown in Equation (22), as well as the observations made, demonstrates the ability to pave the way for future efforts towards theoretically generating the complete Arps' type curves.

Summary and Conclusions

This work has successfully established the missing link between the empirical and the theoretical domains of decline curve analysis for solution-gas drive reservoirs, expressed as a functional relationship between the empirical decline exponent, b_{emp} , and the time-weighted average of the values of the theoretical decline exponent known as \bar{b}_{th} . Theoretical justifications for decline trends in solution-gas drive reservoirs have been offered. For the first time, four distinct rate decline regimes in solution-gas drive reservoirs have been identified. The influence of non-Darcy flow on decline parameter has also been investigated. Analyses have been performed on the sensitivity of the results to some key parameters. Finally, this work has provided mathematical justifications for the existence of the hyperbolic family of curves in decline curve analysis of solution-gas drive reservoirs.

Based on the results presented in this work, the following conclusions are warranted.

1. The theoretical decline parameter, b_{th} , varies considerably through time and reflects the dynamics of the reservoir-fluid interaction through time.
2. The following four distinct regimes of rate decline in solution-gas drive reservoirs have been identified:
 - a. Transient rate decline regime: $b_{th} > 1.0$.
 - b. Transition rate decline regime: $1 > b_{th} > 0.67$.
 - c. Solution-gas drive decline regime: $0.67 > b_{th} > 0.33$.
 - d. Approaching single-phase production: $b_{th} < 0.33$.
3. The effect of non-Darcy flow on decline parameter is insignificant for solution-gas drive reservoirs.
4. The time-weighted average of b_{th} values for a given reservoir/wellbore model is related to the empirical b_{emp} . The equation showing this relationship has been derived and presented in this work.
5. There exists a functional 'agreement' between the empirical and the theoretical domains (as derived in this work) of decline curve analysis for solution-gas drive reservoirs. The best agreement occurs at the time the reservoir has fully spanned the solution-gas drive rate decline regime.
6. Reservoirs with high permeability values may not exhibit the transient rate decline regime as well as the transition rate decline regime.
7. The transient rate decline regime as well as the transition rate decline regime may be absent for wells with small drainage area.
8. The more transient rate decline regime experienced by a well, the higher above 1.0 will be its initial b_{th} values.
9. The relationship between the empirical and the theoretical domains of rate decline analysis derived in this work is also applicable to heterogeneous reservoirs.
10. The hyperbolic decline behaviour of solution-gas drive reservoirs is a direct consequence of the inner boundary con-

dition (constant wellbore pressure) of the dimensionless diffusivity equation for solution-gas drive reservoirs.

Acknowledgements

Computing facilities were provided by the African University of Science and Technology (AUST). Schlumberger donated the simulator suite to AUST. Suggestions from Professor D. Ogbe, Dr. N. Ezekwe, Dr. A. Igbokoyi, Kingsley Akpara, Anthony Ike and Oscar Ogali are also acknowledged.

NOMENCLATURE

A	= Reservoir drainage area, ft ²
a	= Empirical decline parameters
B	= FVF, RB/STB for liquid and RB/SCF for gas
b	= Decline exponent
b_{emp}	= Empirical decline parameter
b_{th}	= Theoretical decline parameter
b_{L-D}	= Decline parameter with non-Darcy considerations
\bar{b}_{th}	= Time-weighted average of b_{th}
c_t	= Total compressibility, psi ⁻¹
D	= The group $(\ln r_e / r_w - 0.75 + s)$
D_i	= Decline parameter, day ⁻¹
h	= Reservoir thickness, ft
i	= Data point position index
k	= Permeability, mD
N	= Non-Darcy flow coefficient, D/STB
P_i	= initial reservoir pressure, psi
\bar{P}	= average reservoir pressure, psi
P_D	= Dimensionless pressure
Pp_D	= Dimensionless pseudo-pressure
q	= Oil flow rate, STB/D
q_{fg}	= Free gas flow rate, STB/D
R_s	= solution gas-oil ratio, SCF/STB
r	= Radius, ft
S_o, S_g	= Saturations, fraction
s	= Skin factor
t	= Time, days
t_o	= Time corresponding to onset of decline, days
$\bar{t}_{AD}, \bar{\bar{t}}_{AD}$	= Dimensionless pseudo-time functions
μ	= viscosity, cP
ϕ	= porosity, fraction


SI Metric Conversion Factors

API ($^{\circ}$ API + 131.5)/141.5	= g/cm ³
bb1 \times 1.589873 E-03	= m ³
cP \times 1.0* E-03	= Pa.s
ft \times 3.048* E-01	= m
ft ² \times 9.290304* E-02	= m ²
$^{\circ}$ F ($^{\circ}$ F - 32)/1.8	= $^{\circ}$ C
mD \times 9.869233 E-04	= μ m ²
psi \times 6.894757 E+00	= KPa

* Conversion factor is exact.

REFERENCES

1. HUBBERT, M.K., Nuclear Energy and the Fossil Fuels; *paper presented at the Spring Meeting of the Southern District Division of the American Petroleum Institute, San Antonio, TX, 7-9 March 1956.*
2. GUO, B., LYONS, W.C. and GHALAMBOR, A., Petroleum Production Engineering, A Computer-Assisted Approach; *Gulf Professional Publishing, Burlington, MA, 2007.*
3. GOLAN, M. and WHITSON, C.H., Well Performance; *2nd Edition, Prentice Hall, 1995.*

4. ARPS, J.J., Analysis of Decline Curves; *Transactions of the AIME*, Vol. 160, pp. 228-247, 1945.
5. FETKOVICH, M.J., Decline Curve Analysis using Type Curves; *Journal of Petroleum Technology*, Vol. 32, No. 6, pp. 1065-1077, June 1980.
6. FETKOVICH, M.J., VIENOT, M.E., BRADLEY, M.D. and KIESOW, U.G., Decline Curve Analysis using Type Curves: Case Histories; *SPE Formation Evaluation*, Vol. 2, No. 4, pp. 637-656, December 1987.
7. COX, D.O., Reservoir Limit Testing Using Production Data; *SPWLA Journal*, Vol. 19, No. 2, pp. 13-17, March-April 1978.
8. EHLIG-ECONOMIDES, C.A. and RAMEY JR., H.J., Transient Rate Decline Analysis for Wells Produced at Constant Pressure; *SPE Journal*, Vol. 21, No. 1, pp. 98-104, February 1981.
9. CAMACHO, V.R. and RAGHAVAN, R., Boundary-Dominated Flow in Solution Gas-Drive Reservoirs; *SPE Reservoir Engineering*, Vol. 4 No. 4, pp. 503-512, November 1987.
10. AHMED, T. and MCKINNEY, P.D., Advanced Reservoir Engineering; *Gulf Professional Publishing, Burlington, MA, 2005*.
11. GENTRY, R.W. and MCCRAY, A.W., The Effect of Reservoir and Fluid Properties on Production Decline Curves; *Journal of Petroleum Technology*, Vol. 30, No. 9, pp. 1327-1341, September 1978.
12. MUSKAT, M. and TAYLOR, M.O., Effect of Reservoir Fluid and Rock Characteristics on Production Histories of Gas-Drive Reservoirs; *Transactions of the AIME*, Vol. 165, No. 1, pp. 78-93, December 1946.
13. ARPS, J.J. and ROBERTS, T.G., The Effect of the Relative Permeability Ratio, the Oil Gravity, and the Solution Gas-Oil Ratio on the Primary Recovery from a Depletion Type Reservoir; *Transactions of the AIME*, Vol. 204, pp. 120-127, 1955.
14. MEAD, H.N., Modifications to Decline Curves Analysis; *Transactions of the AIME*, Vol. 207, pp. 11-16, 1956.
15. MATTHEWS, C.S. and LEFKOVITS, H.C., Gravity Drainage Performance of Depletion-Type Reservoirs in the Stripper Stage; *Transactions of the AIME*, Vol. 207, pp. 265-274, 1956.
16. CAMACHO V., R.G. and RAGHAVAN, R., Some Theoretical Results Useful in Analyzing Well Performance Under Solution Gas Drive; *SPE Formation Evaluation*, Vol. 6, No. 2, pp. 190-198, June 1991.
17. FRAIM, M.L. and WATTENBARGER, R.A., Decline Curve Analysis for Multiphase Flow; *Paper 18274 presented at the SPE Annual Technical Conference and Exhibition, Houston, TX, 2-5 October 1988*.
18. FETKOVICH, M.J., The Isochronal Testing of Oil Wells; *Paper 4529 presented at the Fall Meeting of the Society of Petroleum Engineers of AIME, Las Vegas, NV, 30 September- 3 October 3 1973*.
19. CAMACHO V., R.G. and RAGHAVAN, R., Inflow Performance Relationships for Solution-Gas-Drive Reservoirs; *Journal of Petroleum Technology*, Vol. 41, No. 5, pp. 541-550, May 1989.
20. FREDERICK, J.L. and KELKAR, M., Decline Curve Analysis for Solution Gas Drive Reservoirs; *paper 94859 presented at the SPE Annual Technical Conference and Exhibition, Dallas, TX, 9-12 October 2005*.
21. LEE, J., ROLLINS, J.B. and SPIVEY, J.P., Pressure Transient Testing; *SPE Textbook Series, Volume 9, Society of Petroleum Engineers, Richardson, TX, 2003*. 

$$D = \left(\ln r_D - \frac{3}{4} + s_m \right)$$

With considerations for non-Darcy flow, Equation (A1) applies. Whereas, without considerations for non-Darcy flow, the following applies:

$$q = \frac{kh(\bar{P} - P_{wf})}{141.2\mu B(D)}$$

Hence, it is considered here that the non-Darcy flow effects could be accounted for by replacing D with $D + Nq_{fg}$ in the original derivation presented by Camacho and Raghavan⁽⁹⁾.

The following expressions concerning the solution-gas pseudo-pressure function has been validated and reported⁽⁹⁾.

$$\bar{P}_{pD} = \frac{kh}{141.2q(t)} \int_{\bar{P}(t)}^{P_i} \left(\frac{K_{ro}}{\mu_o B_o} \right) d\bar{P} \dots\dots\dots (A3)$$

$$\bar{P}_{pD} \equiv -D \left[1 - \exp\left(\frac{2\pi \bar{t}_{AD}}{D} \right) \right] \dots\dots\dots (A4)$$

Replacing D with $D + Nq_{fg}$ in Equation (A4), and equating it with the RHS of Equation (A3) after expansion, we obtain

$$\begin{aligned} & \frac{kh}{141.2q(t)} \int_{\bar{P}(t)}^{P_i} \left(\frac{K_{ro}}{\mu_o B_o} \right) d\bar{P} \\ &= -D + D \exp\left(\frac{2\pi \bar{t}_{AD}}{D + Nq_{fg}} \right) - Nq_{fg} + Nq_{fg} \exp\left(\frac{2\pi \bar{t}_{AD}}{D + Nq_{fg}} \right) \dots\dots\dots (A5) \end{aligned}$$

Differentiating Equation (A5) with respect to time:

$$\begin{aligned} & \frac{kh}{141.2} \left[\frac{1}{q} \left(\frac{K_{ro}}{\mu_o B_o} \right) \frac{d\bar{P}}{dt} - \frac{1}{q^2} \frac{dq}{dt} \int_{\bar{P}(t)}^{P_i} \left(\frac{K_{ro}}{\mu_o B_o} \right) d\bar{P} \right] \\ &= \left\{ \frac{(D + Nq_{fg}) 0.006328k \bar{\lambda}}{\phi A \bar{c}_T} \right. \\ & \quad \left. - \bar{t}_{AD} N \frac{dq_{fg}}{dt} \right\} \frac{2\pi D}{(D + Nq_{fg})^2} \exp\left(\frac{2\pi \bar{t}_{AD}}{D + Nq_{fg}} \right) - \left(N \frac{dq_{fg}}{dt} \right) \\ & \quad + \left[N \frac{dq_{fg}}{dt} \exp\left(\frac{2\pi \bar{t}_{AD}}{D + Nq_{fg}} \right) \right] \\ & \quad + \left\{ \frac{(D + Nq_{fg}) 0.006328k \bar{\lambda}}{\phi A \bar{c}_T} \right. \\ & \quad \left. - \bar{t}_{AD} N \frac{dq_{fg}}{dt} \right\} \frac{2\pi Nq_{fg}}{(D + Nq_{fg})^2} \exp\left(\frac{2\pi \bar{t}_{AD}}{D + Nq_{fg}} \right) \dots\dots\dots (A6) \end{aligned}$$

From Reference (9), the following have been derived:

$$\frac{kh}{141.2} \left(\frac{K_{ro}}{\mu_o B_o} \right) \frac{d\bar{P}}{dt} = \frac{2\pi 0.006328k \bar{\lambda}}{\phi A} q \frac{\bar{\lambda}}{\bar{c}_T} \dots\dots\dots (A7)$$

$$\frac{kh}{141.2q} \int_{\bar{P}(t)}^{P_i} \left(\frac{K_{ro}}{\mu_o B_o} \right) d\bar{P} = -D \left[1 - \exp\left(\frac{2\pi \bar{t}_{AD}}{D} \right) \right] \dots\dots\dots (A8)$$

Appendix

Derivation of b_{th-rD} Expression

The total skin factor s_T is considered as:

$$s_T = s_m + Nq_{fg} \dots\dots\dots (A1)$$

Here, the rate term in Equation (A1) is considered to be the rate of the free gas flow in the reservoir, since the free gas is the agent of the turbulence leading to the non-Darcy flow. Incorporating this into the fluid flow equation yields

$$q = \frac{kh(\bar{P} - P_{wf})}{141.2\mu B(D + Nq_{fg})} \dots\dots\dots (A2)$$

Again, accounting for the non-Darcy flow, Equation (A8) yields

$$\frac{kh}{141.2q} \int_{\bar{p}(t)}^{p_i} \left(\frac{K_{ro}}{\mu_o B_o} \right) d\bar{p} = -(D + Nq_{fg}) \left[1 - \exp\left(\frac{2\pi \bar{t}_{AD}}{D + Nq_{fg}} \right) \right] \dots\dots\dots (A9)$$

Substituting Equations (A9) and (A7) into the LHS of Equation (A6),

$$LHS = \frac{2\pi 0.006328k \bar{\lambda}}{\phi A \bar{c}_T} - \frac{1}{q} \frac{dq}{dt} \left\{ -(D + Nq_{fg}) \left[1 - \exp\left(\frac{2\pi \bar{t}_{AD}}{D + Nq_{fg}} \right) \right] \right\} \dots\dots\dots (A10)$$

Rearranging and simplifying the terms on the RHS of Equation (A6) yields the following:

$$RHS = \left\{ -N \frac{dq_{fg}}{dt} \left[1 - \exp\left(\frac{2\pi \bar{t}_{AD}}{D + Nq_{fg}} \right) \right] \right\} + \left[\frac{2\pi 0.006328k \bar{\lambda}}{\phi A \bar{c}_T} \exp\left(\frac{2\pi \bar{t}_{AD}}{D + Nq_{fg}} \right) \right] - \left[\frac{2\pi}{D + Nq_{fg}} \bar{t}_{AD} N \frac{dq_{fg}}{dt} \exp\left(\frac{2\pi \bar{t}_{AD}}{D + Nq_{fg}} \right) \right] \dots\dots\dots (A11)$$

Coupling the entire equation back by equating the LHS and RHS terms, rearranging and simplifying, the following is derived:

$$\frac{1}{q} \frac{dq}{dt} = \frac{1}{D + Nq_{fg}} \left(\frac{2\pi 0.006328k \bar{\lambda}}{\phi A \bar{c}_T} \right) + \frac{N \frac{dq_{fg}}{dt} \left\{ \left[\frac{2\pi \bar{t}_{AD}}{(D + Nq_{fg})} - 1 \right] \exp\left[\frac{2\pi \bar{t}_{AD}}{(D + Nq_{fg})} \right] + 1 \right\}}{(D + Nq_{fg}) \left\{ 1 - \exp\left[\frac{2\pi \bar{t}_{AD}}{(D + Nq_{fg})} \right] \right\}} \dots\dots\dots (A12)$$

Assuming the value of $\frac{2\pi \bar{t}_{AD}}{(D + Nq_{fg})}$ is small enough, the entire numerator of the second term of Equation (A12) can be said to be negligible compared to the first term.

Therefore, Equation (A12) becomes the following:

$$-\frac{1}{q} \frac{dq}{dt} = \frac{1}{D + Nq_{fg}} \left(\frac{2\pi 0.006328k \bar{\lambda}}{\phi A \bar{c}_T} \right) \dots\dots\dots (A13)$$

The assumption above may not be unique to this work. It could be shown that the same assumption is implicitly the condition upon which Equations (7) and (17) of Reference (9) represent for the same quantity, PpD .

Equation (A13) above can be expressed as follows:

$$\frac{1}{d \ln q} = - \frac{\phi A}{2\pi 0.006328k} \left(Nq_{fg} \frac{\bar{c}_T}{\bar{\lambda}} + D \frac{\bar{c}_T}{\bar{\lambda}} \right) \frac{d \ln q}{dt} \dots\dots\dots (A14)$$

Recalling that Arps' exponent b is simply the time derivative of the loss ratio⁽⁴⁾, i.e.,

$$-b_{th-nD} = \frac{d}{dt} \left(\frac{1}{d \ln q} \right)$$

the final expression is obtained thus

$$b_{th-nD} = \frac{\phi A}{2\pi 0.006328k} \left[N \frac{d}{dt} \left(q_{fg} \frac{\bar{c}_T}{\bar{\lambda}} \right) + D \frac{d}{dt} \left(\frac{\bar{c}_T}{\bar{\lambda}} \right) \right]$$

CETI 12-030, **A New Theory for Interpreting Rate Decline Trends in Solution-Gas Drive Reservoirs**. CETI April 2013 1(2): pp. 58-68. Submitted 26 January 2012; Revised 30 October 2012; Accepted 13 March 2013.

Authors' Biographies



Olatunde Mosobalaje holds a B.Tech. degree (2005) in chemical engineering from Ladoko Akintola University of Technology, Ogbomoso, Nigeria, and an M.Sc. degree (2011) in petroleum engineering from the African University of Science and Technology (AUST), Abuja, Nigeria. His current research interests are in reservoir fluid/formation dynamic interactions, rate decline analysis and enhanced oil recovery (EOR) methods.



Dr. Djebbar Tiab is a Senior Professor and Director of International Graduate Programs of Petroleum Engineering at the University of Oklahoma. He received his B.Sc. (1974) and M.Sc. (1975) degrees from the New Mexico Institute of Mining and Technology, and Ph.D. degree (1976) from the University of Oklahoma, all in petroleum engineering, with a minor in mathematics. His research interests include well test analysis, petrophysics and reservoir characterization. Dr. Tiab is the author/co-author of over 200 conference and technical journal papers in the areas of pressure transient analysis, dynamic flow analysis, petrophysics, natural gas engineering, reservoir characterization and reservoir engineering and injection processes. He is the senior author of the textbook *Petrophysics*.